A LFM-based Adaptive Wake-up Signal Detection Approach for Underwater Acoustic Communication System

Haiyu Li[1], Deqing Wang[*,1,2], Yongjun Xie[1], Xiaoyi Hu[1]
1. Key Laboratory of Underwater Acoustic Communication and Marine Information Technology (Xiamen University), Ministry of Education, Xiamen, Fujian, China
2. Key Laboratory of Technology and Application For Safeguarding of Marine Rights and Interests, SOA, Guangzhou, Guangdong, China
23320171153118@stu.xmu.edu.cn, {deqing, xyj, xyhu}@xmu.edu.cn

ABSTRACT

The paper focuses on wake-up mechanism for underwater acoustic communication (UAC) system. Wake-up mechanisms for UAC terminals play an important role in reducing the power consumption and extending the battery life. Compared with terrestrial wireless counterparts, the wake-up receivers for UAC terminals are challenged by the severe underwater acoustic channels, which are characterized by doubly-selective fading and low signal-to-noise ratio (SNR). Furthermore, the wake-up receiver is with weak processing ability. The paper proposes a wake-up mechanism named as channel-adaptive detection and joint decision (ChAD-JD). ChAD-JD uses linear frequency modulation (LFM) as wake-up signals. In order to increase the detection probability and reduce the probability of false alarm, the novel approach applies channel-adaptive detection and joint decision methods, respectively. Simulation and experimental results show that ChAD-JD is more reliable and effective compared with traditional LFM-based detection methods with a fixed threshold.

CCS CONCEPTS

• **Underwater communications**; • **Underwater experimentation and deployments**;

KEYWORDS

underwater acoustic communication, LFM, wake-up, channel-adaptive detection, joint decision

∗ The corresponding author.

WUWNet'18, December 3–5, 2018, Shenzhen, China

ACM ISBN 978-1-4503-6193-4/18/12...$15.00
https://doi.org/10.1145/3291940.3291962

1 INTRODUCTION

Underwater acoustic communication (UAC) or underwater acoustic sensor networks (UASNs) have attracted much research interest in recent years because of their wide range of potential applications, such as marine resources exploitation, industrial instrumentation and control, military surveillance, and security monitoring [4, 8]. Compared with the terrestrial wireless communication or networks system, energy efficiency becomes even more critical for UAC or UASNs where underwater acoustic terminals rely on non-rechargeable and unchangeable batteries to provide essential power for long-term sensing, data collection, and communications [20]. Therefore, it is important to develop effective power saving mechanisms for underwater acoustic terminals so that energy conservation can be achieved and the lifetime of UASNs can be extended.

Among existing power saving mechanisms, wake-up mechanisms for UAC terminals plays an important role in reducing the power consumption and extending the battery life. UAC terminals with wake-up ability just consume a little energy when they stay in the idle listening mode. However, the design of underwater acoustic wake-up mechanism is challenged by the severe underwater acoustic channels, which are characterized by time-varying multi-path, severe Doppler effect and high ambient noise. Some extraordinary wake-up mechanisms are necessary to combat the effect of doubly-selective fading and low signal-to-noise ratio (SNR) [14]. Furthermore, compared with frame synchronization, the wake-up mechanisms are usually based on low power devices with weak processing ability.

A low-power and low-complexity solution is to convert the carrier and ID detection IC AS3933 to handle acoustic hydrophone inputs [17]. The chip AS3933 is a commercial integrated circuit which is designed for active RFID tags with a low power consumption. It will be waken-up if the particular carrier has been sensed. However, the AS3933 is not suitable to combat multi-path inter-symbol interference (ISI) channel for it is lack of any built in mechanisms to deal with the ISI. Applying the same wake-up signal, a single-frequency, a design of low-power wake-up circuits based on SCM C8051F020 has been proposed in [5]. The circuits collect the wake-up signal and identify the frequency by making single point of fixed-point Discrete Fourier Transform (DFT). But the simulation results are just discussed in Gaussian white noise channels. The authors in [23] propose a low-complexity wake-up receiver using a TI MCU named as MSP430F5529 for UASNs. By using dual pseudorandom noise (PN) sequences, the wake-up mechanism is designed based on auto-correlation to reduce the complexity. The proposed dual PN detection scheme has been tested in long multi-path channels with more than 60 taps. However, the time-selective characteristics of underwater acoustic channel destroys the auto-correlation properties of PN sequences, resulting in low detection rate.

Differently from single-frequency or PN sequences, linear frequency modulation (LFM) signals have been used for frame synchronization [7, 19, 22], random access [13], communication [3, 11] and parameter estimation [16, 24] due to its good autocorrelation and Doppler tolerance in doubly-selective fading channels. Traditional detection methods for LFM signals are based on a replica correlation detector [2, 6]. The LFM signal is assumed to have been received when the correlation coefficient between the received signal and the local signal is higher than the threshold. In order to separate the overlapping LFM signals, a method based on fractional Fourier transform (FrFT) is applied in all kinds of signal processing applications. FrFT is a generalization of the classical Fourier transform and can be interpreted as a rotation in the time-frequency plane. In the FrFT domain, an LFM signal can be represented as an impulse at an appropriate time-frequency rotation angle since the transform kernel is a set of chirp bases [1]. However, the FrFT-based detection methods are much more complexity than traditional correlation-based ones, resulting in computational burden for wake-up receivers with weak processing ability. Furthermore, the detection rate is a more important performance criteria rather than accurate parameters estimation in wake-up mechanisms.

Constant false alarm rate (CFAR) detector is widely used in radar or sonar detection. CFAR system has the ability to change its threshold adaptively as the ambient noise changes[9, 10, 18]. In this paper, we adopted this idea and further improved it to achieve better detection performance.

In this paper, we propose a novel LFM-based wake-up signal detection approach named as channel-adaptive detection and joint decision (ChAD-JD) for UAC system. ChAD-JD focuses on increasing detection probability and reducing the probability of false alarm according to the channel states. Its main characteristics are listed as follows.

• Compared with traditional LFM-based detection methods only applying a fixed threshold, ChAD-JD uses compound detection conditions to get the correlation peak locations except a fixed threshold. The channel states are embedded in the compound conditions to increase detection probability, which is why the detection approach is called channel-adaptive one.

• In order to reduce the probability of false alarm, L adjacent LFM signals are transmitted in the sender side and an additional joint judging method is applying after getting correlation peak locations.

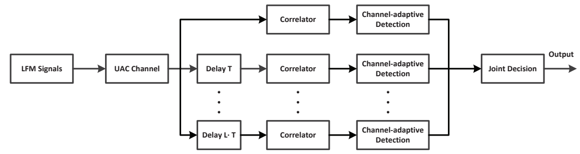

Figure 1: System model

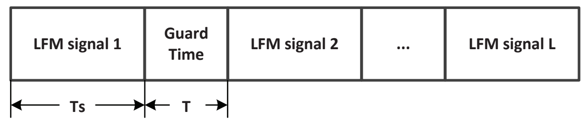

Figure 2: Signal structure

The rest of the paper is organized as follows. Section 2 describes the system model and the wake-up signal selection. In Section 3, We introduce the novel wake-up signal detection approach. Simulation and experimental results are provided in Section 4. Finally, conclusions are given in Section 5.

2 SYSTEM MODEL

In this paper, LFM signal is selected as the basal wake-up signal. The complex envelope LFM signal is given by:

$$s(t) = \frac{1}{\sqrt{T_s}} rect(\frac{t}{T_s}) e^{j\pi\mu t^2}, \tag{1}$$

where $rect(\frac{t}{T_s})$is a rectangular window function. T_s is the width of the rectangular window function, $\mu = \frac{B}{T_s}$ is the frequency rate, and B is the bandwidth. The ambiguity function of positive slope LFM signal is given by:

$$c(\tau, f_d) = \left| (1 - \frac{|\tau|}{T_s}) sinc[\pi T_s(\mu\tau + f_d)(1 - \frac{|\tau|}{T_s})] \right|^2, \tag{2}$$

where τ is the multipath time-delay and f_d is the Doppler frequency shift. According to the LFM ambiguity function, we can get that[7]:

• LFM signals have good autocorrelation and spectral characteristics.

• LFM signals' ambiguity function is blade or ridge, and have good resolution.

• Good peak-to-average power ratio characteristics.

In a word, the LFM signal has the characteristics of high processing gain, strong anti-interference ability and stable performance. Moreover, it has an important feature that it has high Doppler tolerance, so it is widely used as a wake-up or synchronization signal in various underwater acoustic communication systems [12, 13, 19, 21, 22].

The system model is shown in Fig.1. The transmitter sends a wake-up signal consisting of L LFM signals as shown in Fig.2. After these signals pass through the UAC channel,

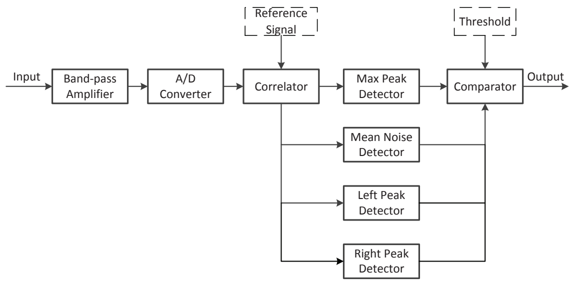

Figure 3: Channel-adaptive detection diagram

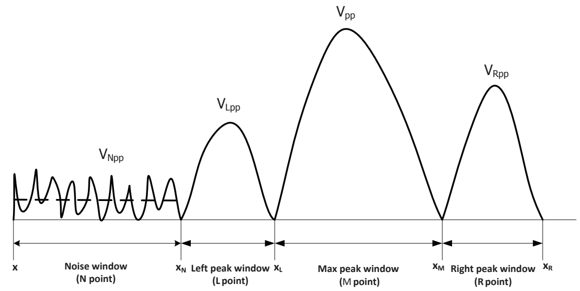

Figure 4: LFM peak detection windows

they are correlated to the reference signal by Replica Correlation(RC) detector at guard time intervals T in order.

The UAC channel consists of N_{pa} discrete path is given by:

$$h(t,\tau) = \sum_{p=1}^{N_{pa}} A_p(t)\delta(\tau - \tau_p(t)), \tag{3}$$

where $A_p(t)$ and $\tau_p(t)$ are the time-varying amplitude and delay for the pth path, respectively. The discrete form of the $h(t,\tau)$ is defined as $h(n;k)$ and $s(n)$ is the discrete form of transmitted signal $s(t)$. The received signal can be expressed by the linear time varying convolution of $s(n)$ and $h(n;k)$ in the presence of additive white Gaussian noise(AWGN) $z(n)$ [15]:

$$r(n) = \sum_{k=0}^{K-1} h(n;k)s(n-k) + z(n), \tag{4}$$

where $r(n)$ denote the nth received signal, and K is the delay taps. According to [6], the result after RC detector is given by:

$$y(n) = \left| \sqrt{\frac{2}{N}} \sum_{i=0}^{N-1} s^*(i)r(i+n) \right|^2, \tag{5}$$

where N is the length of $r(n)$. After $r(n)$ passes through the RC detector, the channel-adaptive detector which will be described in 3.1 is used to find the location of LFM correlation peak. The LFM correlation peak location X_i are given by:

$$X_i = \arg\max(y(n)) \qquad n \in [(i-1)m, m], \tag{6}$$

where $i = 1, ..., L$ is the number of LFM, and m is the length of single LFM autocorrelation. Then we have L LFM locations and the results will be used in joint decision to decided whether the system wake up or not. We define the UAC wake-up state as X_{out}, and the joint decision system function described in 3.2 as $f(x)$. Then we have:

$$X_{out} = f(X_1, ..., X_L), \tag{7}$$

where $X_{out} = 1$ means UAC system wakes up successfully.

According to the system model, this paper focuses on the channel-adaptive detection and joint decision.

3 DETECTION APPROACHES

3.1 Channel-adaptive Detection

Traditional LFM detection approach use the single threshold detection method to search LFM signals. If the SNR of the receiver is relatively high, the LFM signal can be detected as long as the correlation peak value of the LFM signal is larger than the set threshold value. However, this method is ineffective in the case of low SNR. In order to satisfy the actual demand, we propose the new dynamic threshold decision approach.

As shown in Fig.3, in order to search for the LFM correlation peak, four different detectors are used to find four variables. Then, these variables pass through the comparator to compose the dynamic threshold and they will help find the LFM correlation peak. These variables are defined as V_{Npp}, V_{Lpp}, V_{pp} and V_{Rpp}, which are given by:

$$\begin{aligned} V_{Npp}(x) &= \frac{1}{N}\sum y(n) \quad n \in [x, x_N - 1] \\ V_{Lpp}(x) &= \max(y(n)) \quad n \in [x_N, x_L - 1] \\ V_{pp}(x) &= \max(y(n)) \quad n \in [x_L, x_M - 1] \\ V_{Rpp}(x) &= \max(y(n)) \quad n \in [x_M, x_R - 1] \end{aligned} \tag{8}$$

where x is the search starting point, $x_N = x + N, x_L = x_N + L, x_M = x_L + M, x_R = x_M + R$.

As shown in Fig.4, V_{Npp} is defined as the average noise value, which means it is the average of all the values in the N-point *noise window*. V_{pp} is the maximum value of the M-point *max peak window*, which is used to look for LFM peak. V_{Lpp} and V_{Rpp} are the impulse noise peaks of the L-point *left peak window* and R-point *right peak window* on the both sides of the V_{pp}, respectively.In order to combat multipath interference, M should be long enough to cover the whole received signals affected by multipath effect. N should be long enough to reflect the noise average level. To reflect part impulse noise peak, L, R should not be longer than M. According to Section 4.1, Typical values of N, L, M, R are 3200, 200, 1600, 200, respectively.

After these windows begin sliding the correlation values we would have $V_{Npp}(x)$, $V_{Lpp}(x)$,$V_{Rpp}(x)$ and $V_{pp}(x)$, which means each search point x corresponds to 4 different parameters. The threshold is defined as V_{th} and we define whether the LFM correlation peak is detected as D. Then there are:

$$\begin{aligned}
&D = 1, X = x; \\
&s.t. \\
&C1 : V_{pp}(x) > \alpha \bullet V_{Npp}(x) \qquad (9) \\
&C2 : V_{pp}(x) > \beta \bullet V_{Lpp}(x) \cap V_{pp}(x) > \beta \bullet V_{Rpp}(x) \\
&C3 : V_{pp}(x) > V_{th}
\end{aligned}$$

where $D = 1$ means LFM correlation peak has been found, X is the LFM correlation peak location, and α and β are the multiple coefficients of mean noise value and both sides peak, respectively. α and β are set to make the LFM correlation peak's judgment more accurate. According to Section 4.1, Typical values of α, β and v_{th} are 2, 2, 0.6, respectively.

It can be seen from above condition that $C1$ and $C2$ make up the dynamic threshold which would change with the noise level. Together with the traditional settled threshold, it can effectively reduce the wake-up false alarm probability under low SNR conditions.

The above approach can be described as the following Algorithm 1.

Algorithm 1 Channel-adaptive Detection

Initialization:
$INPUT \quad V_{Th}, N, L, M, R, \alpha, \beta, D, and\, x.$
$Set \quad x_N = x + N, x_L = x_N + L, x_M = x_L + M, x_R = x_M + R$
Iteration:
for $x = 1 : lengthof(y(n))$ **do**
  for $n = x : x_N - 1$ **do**
    $V_{Npp}(x) = \frac{1}{N}\sum y(n)$
  end for
  for $n = x_N : x_L - 1$ **do**
    $V_{Lpp}(x) = \max(y(n))$
  end for
  for $n = x_L : x_M - 1$ **do**
    $V_{pp}(x) = \max(y(n))$
  end for
  for $n = x_M : x_R - 1$ **do**
    $V_{Rpp}(x) = \max(y(n))$
  end for
  if $V_{pp}(x) > \alpha \bullet V_{Npp}(x)$ **then**
    if $V_{pp}(x) > \beta \bullet V_{Lpp}(x) \bigcap V_{pp}(x) > \beta \bullet V_{Rpp}(x)$ **then**
      if $V_{pp}(x) > V_{Th}$ **then**
        $D = D + 1, X_D = x$
      end if
    end if
  end if
end for
$OUTPUT \quad X$

3.2 Joint Decision

Channel-adaptive detection may lead to missed detection due to the fading channel. In order to improve the reliability, the paper proposes a kind of joint decision mechanism in addition to the Channel-adaptive detection one mentioned in Sec.3.1. It's known to all that there are $M(0 \leq M \leq L)$ LFM correlation peaks after Channel-adaptive detection. Then we focus on the problem that how to get wake-up result from M LFM correlation peaks in this section. For the sake of description, we choose L as 3.

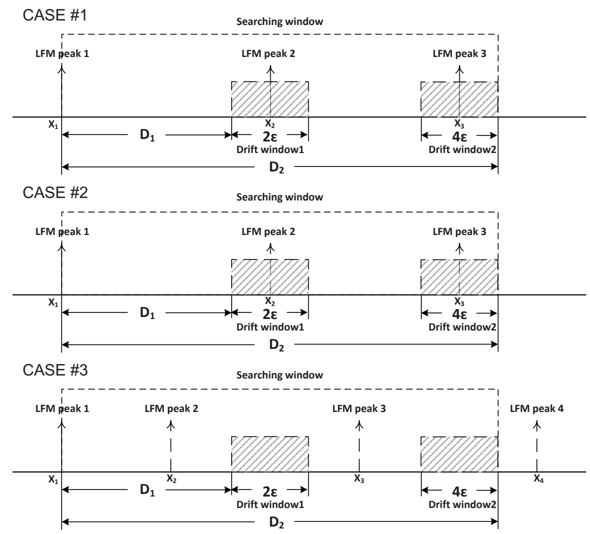

Figure 5: Joint decision diagram

Suppose an ideal situation, named as Case ♯1, which is shown in Fig.5. In this situation, all peaks were detected, the locations for these peaks may drift in a short window due to Doppler effect. The width of the drift windows are denoted as 2ε *and* 4ε, respectively. As long as two among three peaks are detected, the system will output wake-up instruction. Obviously, the *right* peaks should satisfy a specific gap length between the first and following LFM peak locations. Each joint decision is based on the LFM peaks in the searching window. The first LFM peak location is used as the start point of the searching window. The width between the first LFM signal to the third LFM signal is $2T_s + 2T$, so the searching window is set to $D_2(D_2 = 2T + 2T_S + 2\varepsilon)$, under the Doppler effect. The drift windows should cover the correct position where the *right* LFM peak may occur. Under Doppler effect, the with between X_1 to drift window 1 is $D_1(D_1 = T + T_S - \varepsilon)$ and the with between X_1 to drift window 2 is $2D_1$. In Case ♯1, once the first LFM peak has been detected, the searching window is used to look for following LFM peaks. Fortunately, the second LFM peak is in drift window 1 and the third LFM peak is in drift window 2, which means they are in the right place and the UAC system will be waked up.

There are two non-ideal situations, named as Case ♯2 and Case ♯3, respectively. Case ♯2 shows the missed detection situation. In this situation, after the first LFM has been detected, there are only one LFM peak in the drift windows. For example, as the Fig.5 shows, the second LFM peak is found in drift window 1 and the third LFM peak is missing or the third LFM peak is found in drift window 2 and the second LFM peak is missing(Different dotted arrows indicate different situations). However, because two among three peaks are detected, the UAC system will still wake up successfully in this situation.

Case ♯3 shows the false-alarm detection situation. In this situation, after the first LFM has been detected, the second LFM peak location is outside drift window 1 and 2 like $X_2, X_3, or\ X_4$ in the figure. In this situation, the first LFM peak location X_1 will be abandoned, the second LFM peak location $X_2, X_3 or X_4$ will be selected as a new starting point. The searching window would also start from the new starting point. Then, the joint decision continue to make a judgment based on the Case ♯1 and ♯2. After all the LFM peak locations pass through the joint detector, the UAC system will decide to wake up or not according to the results.

The joint decision approach could improve wake-up performance at low SNR. Successful wake-up is defined as $Y = 1$,then the approach can be conclude as following Algorithm 2.

Algorithm 2 Joint Decision

Initialization:
$INPUT \quad X_1, ..., X_M, \varepsilon, T, T_S.$
$Set \quad D_1 = T + T_S - \varepsilon, D_2 = 2T + 2T_S + 2\varepsilon, state = 0$
Iteration:
while $state == 0$ **do**
  if $X_1 + D_1 \le X_2 \le X_1 + D_1 + 2\varepsilon$ **then**
    $state = 1$
  else
    if $X_1 + 2D_1 \le X_2 \le X_1 + 2D_1 + 4\varepsilon$ **then**
      $state = 1$
    else
      $state = 0$
      for (i=1:M) **do**
        $X_i = X_{i+1}, M = M - 1$
      end for
    end if
  end if
  if $state == 3$ **then**
    $OUTPUT \quad Y = 1$
  end if
end while

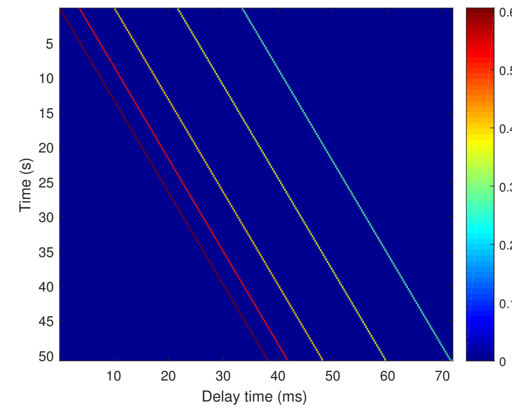

Figure 6: Channel impulse state for simulation

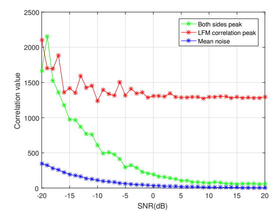

(a) Correlation values

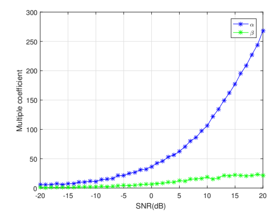

(b) $\alpha - \beta$

Figure 7: $\alpha - \beta$ comparison with different SNRs

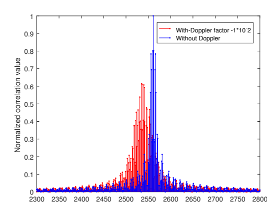

(a) Doppler effect

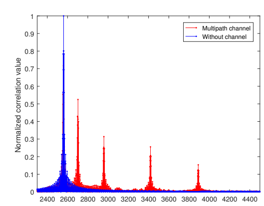

(b) Multipath effect

Figure 8: Correlation result with Doppler or Multipath effect

4 SIMULATION AND EXPERIMENT RESULT

In this section, We explore the performance of the aforementioned methods through simulation experiments and sea trial experiments.

4.1 Simulation Result

In this section, the proposed wake-up mechanism ChAD-JD is evaluated by computer simulation. The wake-up signal is consisted of 3 adjacent identical LFM symbols separated by a guard interval with the length of $T = 32$ ms. The parameters of the transmitted LFM symbol in the simulation are assumed as follows. The frequency band ranges from 2.5kHz to 5.5kHz. The time duration is set to be $T_s = 64$ms. The signal sampling rate is 40kHz. So, there are 2560 samples for each LFM symbol. The channel used in simulation is shown in Fig.6. Fig.7 shows the simulation of LFM correlation peaks, mean noise and both sides peak at different SNR. From Fig.7, the values of α and β under different SNR can be determined, and it can be seen from Fig.7b that as the SNR increases, α and β also increase. Fig.7 can be used to optimise the values of α and β to increase the probability of

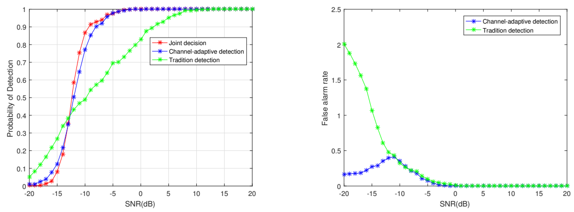

(a) Probability of detection **(b) False alarm rate**

Figure 9: Detection performance with different threshold

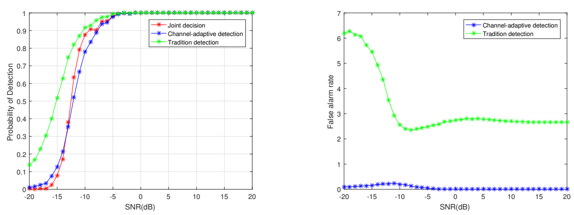

(a) Probability of detection **(b) False alarm rate**

Figure 10: Detection performance with low threshold

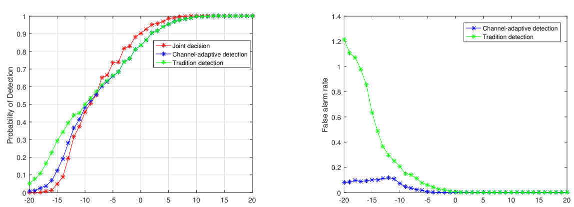

(a) Probability of detection **(b) False alarm rate**

Figure 11: Detection performance with high threshold

detection (PD) while reducing the false alarm rate (FAR). Fig.8a is the correlation result of a single LFM signal passing through the Doppler channel. It can be seen from the figure that the Doppler effect causes signal peak drift, so the drift window is used in joint decision. Fig.8b is a correlation result of a single LFM signal pass through the channel shown in Fig.6. It can be seen from the figure that the multipath extension point range is 1332 points, in which case M should be more than 1332. When the multipath effect is more serious, a larger M value should be used. If M is smaller than the multipath expansion, the condition C2 may not be satisfied and that will cause miss-detection. The parameters are set as follows:$\alpha = 4, \beta = 2, N = 3200, L = R = 200, M = 1600, \varepsilon = 50$ based on aforementioned result.

Fig.9, Fig.10 and Fig.11 show the simulation experiment results of the channel-adaptive detection and joint decision and tradition detection under different threshold, respectively. There are 1000 experiments per SNR. Here the PD and FAR is given by:

$$\begin{aligned} PD &= \frac{N_D}{Num} \\ FAR &= \frac{N_F}{Num} \end{aligned} \tag{10}$$

where N_D is the number of detected wake-up signals, N_F is the number of false alarm signals and Num is the number of transmitted wake-up signals.

Fig.9 shows the detection performance under different thresholds. The normalized threshold of ChAD-JD is 0.6 and the normalized threshold of the tradition detection is 0.9. The result shows that the performance of ChAD-JD is better than the tradition detection in low SNR. In the case of extremely low SNR, the PD of the tradition detection is higher than the others but it's FAR is also rather higher.

Fig.10 shows the detection performance under low thresholds. The normalized thresholds are set to 0.6 in those detections. The result shows that the tradition detection PD is a little higher than ChAD-JD while it's FAR is quite higher. So the performance of tradition detection is worse than the others.

Fig.11 shows the detection performance under high thresholds. The normalized thresholds are set to 0.9. In this case, the PD of different detection is similar but the FAR of tradition detection is higher than ChAD. The performance of ChAD-JD with high threshold is poor than ChAD-JD with low threshold.

There is a phenomenon in the simulations that the FAR of ChAD is non-monotonic. The reason is that a successful detection needs to satisfy 3 conditions according to Eq.9. When the SNR is extremely low, the false alarm signals satisfy C3 but does not satisfy C1 and C2. As the SNR gradually increases, the false alarm signals satisfy 3 conditions at the same time, causing an erroneous judgement and FAR increasing. When the SNR rises to a certain extent, the false alarm signals don't satisfy C3, and the FAR decreases as the SNR increases.

To sum up, ChAD-JD performance is better than tradition detection. The ChAD-JD get the best performance in low threshold. The PD of joint decision is similar to channel-adaptive detection. But joint decision is more credible than channel-adaptive detection since it's success conditions are more demanding and that could reduce false alarm.

The experimental results show that under the low SNR, ChAD-JD can improve the success rate of wake-up. On the other hand, using ChAD-JD can effectively prevent other noise signal interference and improve the credibility of wake-up.

4.2 Experimental result

Fig. 12 shows the deployment of sea trial at Taiwan Strait in July,2014. The distance between the sender and the receiver is 30 km and the depth is 50 m. The transmitter and receiver were deployed at the depth of 30 m . The wind speed

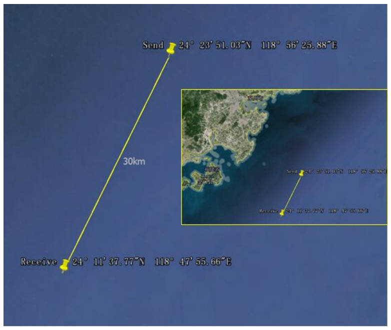

Figure 12: Deployment of sea trial at Taiwan Strait in July, 2014

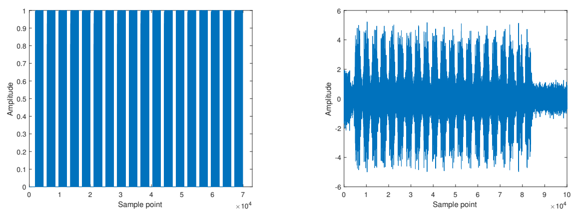

(a) Transmitted signal **(b) Received signal**

Figure 13: Transmitted and received signals

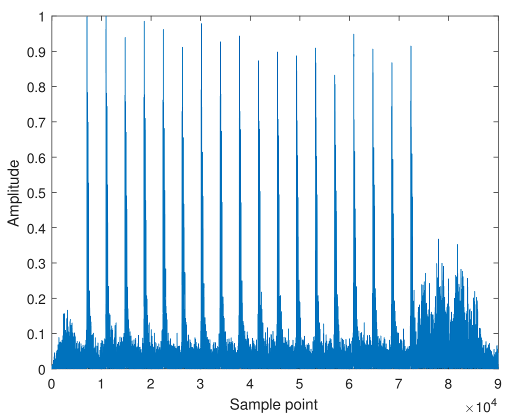

Figure 14: Correlation outputs

is from 5 to 11 m/s, which is equivalent to the scale level of 3 to 5.The experimental data is collected by the NI acquisition card and subsequently processed by Matlab.The single LFM signal format is the same as the above simulation, and 18 LFM signals are transmitted at one time with the same interval. Fig. 13 shows transmitted signals and received signals. Each time an LFM signal is shifted as a new start, and three LFM signals are constructed as a group, theoretically, 16 groups of wake-up signals can be constructed, so that up to 16 wake-up can be detected. The parameter settings

Table 1: Sea trail result

No.	LFM sent	ChAD-JD	Tradition
1	18	16	18
2	18	16	18
3	18	16	18
4	18	16	20
5	18	16	41
6	18	16	18
7	18	16	28
8	18	16	29
9	18	16	26
10	18	16	17

used in the experiment are consistent with the simulation experiments.

Fig. 14 shows the correlation output results of a sea trial. Finally, 10 groups of signals are transmitted and received. The result after ChAD-JD are given in the table 1.

TABLE 1 shows the results of 10 sea trials. A total of 180 LFM signals were sent to form 160 sets of ChAD-JD wake-up signals, and a total of 160 wake-ups were detected using ChAD-JD. While a total of 233 wake-ups were detected using tradition method. The experimental results show that the ChAD-JD is valid and can reduce the probability of false alarm compared to tradition wake-up method.

5 CONCLUSIONS

In this paper, in order to solve the wake-up problem in underwater acoustic communication, we propose a channel-adaptive detection method using LFM signal. Based on this, a joint decision mechanism is proposed. Simulation experiments and sea trials show that the proposed method can effectively improve the PD and reduce PFA of wake-up compared to traditional method applying a fixed threshold.

6 ACKNOWLEDGMENTS

The work is supported by key laboratory open subject funding from Key Laboratory of Technology and Application For Safeguarding of Marine Rights and Interests, SOA (Grant No. 1708). Deqing WANG is also supported by the Research Fund for the Visiting Scholar Program by the China Scholarship Council (Grant No. 201506315026).

REFERENCES

[1] Luis B Almeida. 1994. The fractional Fourier transform and time-frequency representations. *IEEE Transactions on signal processing* 42, 11 (1994), 3084–3091.

[2] Paul M Baggenstoss. 1994. On detecting linear frequency-modulated waveforms in frequency-and time-dispersive channels: Alternatives to segmented replica correlation. *IEEE Journal of Oceanic Engineering* 19, 4 (1994), 591–598.

[3] Yun Chen, Yilin Wang, Jidan Mei, and Ping Cai. 2011. Research on positive and negative slope LFM signal joint coding communication technology based on fractional Fourier transform. In *Advanced Computer Control (ICACC), 2011 3rd International Conference on*. IEEE, Harbin, China, 362–366.

[4] Mandar Chitre, Shiraz Shahabudeen, Lee Freitag, and Milica Stojanovic. 2008. Recent advances in underwater acoustic communications & networking. In *OCEANS 2008*. IEEE, Quebec City,Canada, 1–10.
[5] Zhang Cuixia, Wu Jiaxin, and Li Yuanxuan. 2012. Design of Low-power Wake-up Circuits in Underwater Acoustic Communication. *Physics Procedia* 33 (2012), 884–891.
[6] Benjamin Friedlander and Ariela Zeira. 1996. Detection of broadband signals in frequency and time dispersive channels. *IEEE Transactions on signal processing* 44, 7 (1996), 1613–1622.
[7] Zheng Guo, Shefeng Yan, and Lijun Xu. 2016. A new method for frame synchronization in acoustic communication. In *OCEANS 2016*. IEEE, Shanghai, China, 1–6.
[8] Himanshu Jindal, Sharad Saxena, and Singara Singh. 2015. Challenges and issues in underwater acoustics sensor networks: A review. In *International Conference on Parallel, Distributed and Grid Computing*. Solan, India, 251–255.
[9] M. A. Khalighi and M. H. Bastani. 2000. Adaptive CFAR processor for nonhomogeneous environments. *IEEE Transactions on Aerospace & Electronic Systems* 36, 3 (2000), 889–897.
[10] Hyeonsu Kim, Jongpil Seo, Jongmin Ahn, and Jaehak Chung. 2017. Snapping shrimp noise mitigation based on statistical detection in underwater acoustic orthogonal frequency division multiplexing systems. *Japanese Journal of Applied Physics* 56, 7S1 (2017), 07JG02.
[11] Wangwei Lei, Deqing Wang, Yongjun Xie, Bingbing Chen, Xiaoyi Hu, and Huabin Chen. 2012. Implementation of a high reliable chirp underwater acoustic modem. In *Oceans 2012*. IEEE, Yeosu, South Korea, 1–5.
[12] Guolong Liang, Nan Zou, Jin Fu, and Jinjin Wang. 2014. Robust underwater acoustic remote control method. In *IEEE International Conference on Signal Processing, Communications and Computing*. Guilin, China, 919–922.
[13] Rothna Pec, Mohammed Saquib Khan, and Yong Soo Cho. 2017. An LFM-based preamble for underwater communication. In *Information and Communication Technology Convergence (ICTC), 2017 International Conference on*. IEEE, Jeju, South Korea, 1181–1183.
[14] Parastoo Qarabaqi and Milica Stojanovic. 2013. Statistical characterization and computationally efficient modeling of a class of underwater acoustic communication channels. *IEEE Journal of Oceanic Engineering* 38, 4 (2013), 701–717.
[15] Fengzhong Qu and Liuqing Yang. 2010. On the estimation of doubly-selective fading channels. *IEEE Transactions on Wireless Communications* 9, 4 (2010), 1261–1265.
[16] Huan Ren, Xiaoyi Hu, Fang Xu, Xieyong Jun, Wangde Qing, Chaowu Zhan, and Yanglong Chen. 2014. SNR estimation algorithm of LFM signal based on FRFT for long range and shallow underwater acoustic communication systems. In *OCEANS 2014*. IEEE, TAIPEI, 1–6.
[17] Antonio Sánchez, Sara Blanc, Pedro Yuste, and Juan José Serrano. 2011. RFID based acoustic wake-up system for underwater sensor networks. In *2011 Eighth IEEE International Conference on Mobile Ad-Hoc and Sensor Systems*. IEEE, Valencia, Spain, 873–878.
[18] Tri Budi Santoso, Miftahul Huda, and Hani'Ah Mahmudah. 2016. Performance evaluation of CFAR detector for delay spread analysis of underwater acoustic channel. In *Electronics Symposium*. 173–177.
[19] Haitao Su, Xiaomei Xu, Yi Tao, Yougan Chen, and Xiaokang Zhang. 2014. Frequency-hopping acoustic communication in shallow water: Synchronization with time-reversal and united frame structure. In *OCEANS 2014*. IEEE, TAIPEI, 1–5.
[20] Ruoyu Su, Ramachandran Venkatesan, and Cheng Li. 2016. An energy-efficient asynchronous wake-up scheme for underwater acoustic sensor networks. *Wireless Communications and Mobile Computing* 16, 9 (2016), 1158–1172.
[21] Haixin Sun, Xu Ru, and Xu Fang. 2007. A New Accurate Symbol Synchronization Scheme for underwater acoustic communication systems. In *IEEE International Workshop on Anti-Counterfeiting, Security, Identification*. 336–339.
[22] Yongjun Xie, Xiaoyi Hu, Jing Xiao, Deqing Wang, and Wangwei Lei. 2009. Implementation of timing synchronization for OFDM underwater communication system on FPGA. In *Anti-counterfeiting, Security, and Identification in Communication, 2009. ASID 2009. 3rd International Conference on*. IEEE, Hong Kong, China, 568–570.
[23] Ming Yue, Y Rosa Zheng, Zhenrui Chen, and Yunfeng Han. 2016. Microcontroller implementation of low-complexity wake-up receiver for wireless sensor nodes in severe multipath fading channels. In *Ocean Acoustics (COA), 2016 IEEE/OES China*. IEEE, Harbin, China, 1–6.
[24] Yanbo Zhao, Hua Yu, Gang Wei, Fei Ji, and Fangjiong Chen. 2016. Parameter Estimation of Wideband Underwater Acoustic Multipath Channels based on Fractional Fourier Transform. *IEEE Trans. Signal Processing* 64, 20 (2016), 5396–5408.